PHILOSOPHICAL TRANSACTIONS OF THE ROYAL SOCIETY A MATHEMATICAL, PHYSICAL & ENGINEERING SCIENCES

The Structure of the Near-Wall Region of Two-Dimensional Turbulent Separated Flow

Roger L. Simpson

Phil. Trans. R. Soc. Lond. A 1991 **336**, 5-17
doi: 10.1098/rsta.1991.0063

The structure of the near-wall region of two-dimensional turbulent separated flow

By Roger L. Simpson

Department of Aerospace and Ocean Engineering, Virginia Polytechnic Institute and State University, Blacksburg, Virginia 24061, U.S.A.

The time-dependent structure of the wall region of separating, separated, and reattaching flows is considerably different than that of attached turbulent boundary layers. Large-scale structures, whose frequency of passage scales on the freestream velocity and shear layer thickness, produce large Reynolds shearing stresses and most of the turbulence kinetic energy in the outer region of the shear layer and transport it into the low velocity reversed flow next to the wall. This outer flow impresses a near wall streamwise streaky structure of spanwise spacing λ_z simultaneously across the wall over a distance of the order of several λ_z. The near wall structures produce negligible Reynolds shear stresses and turbulence kinetic energy.

1. Introduction

The wall flow behaviour of nominally two-dimensional separated turbulent boundary layers is considerably different than that of attached turbulent boundary layers. To begin with, the usual 'law-of-the-wall' mean velocity profile for attached flow does not usually apply to the mean backflow velocity profile. Local turbulence intensities are large, so the mean flow is not an approximation to the instantaneous flow behaviour. Consequently, it is worthwhile to include here some features of the mean backflow while discussing the time-dependent instantaneous flow structure. Earlier of my reviews (Simpson 1985, 1987, 1989) discuss in detail prior experimentation and computational work, a review of calculation methods, and a summary of our understanding of the physical behaviour of two-dimensional turbulent separated flows, respectively. The emphasis here is on the time-dependent flow structure near the wall.

By *separation*, we mean the entire process of *departure* or *breakaway*, or the breakdown of the boundary-layer flow (Sears & Telionis 1975). An abrupt thickening of the rotational-flow region next to a wall and significant values of the normal-to-wall velocity component must accompany breakaway, or otherwise this region would not have any significant interaction with the free-stream flow. This unwanted interaction causes a reduction in the performance of the flow device of interest (e.g. a loss of lift on an airfoil or a loss of pressure rise in a diffuser).

It is too narrow a view to use vanishing surface shearing stress or flow reversal as the criterion for separation. Only in steady two-dimensional flow do these conditions usually accompany separation. In unsteady two-dimensional flow the surface shear stress can change sign with flow reversal without the occurrence of breakaway.

Phil. Trans. R. Soc. Lond. A (1991) **336**, 5–17
Printed in Great Britain

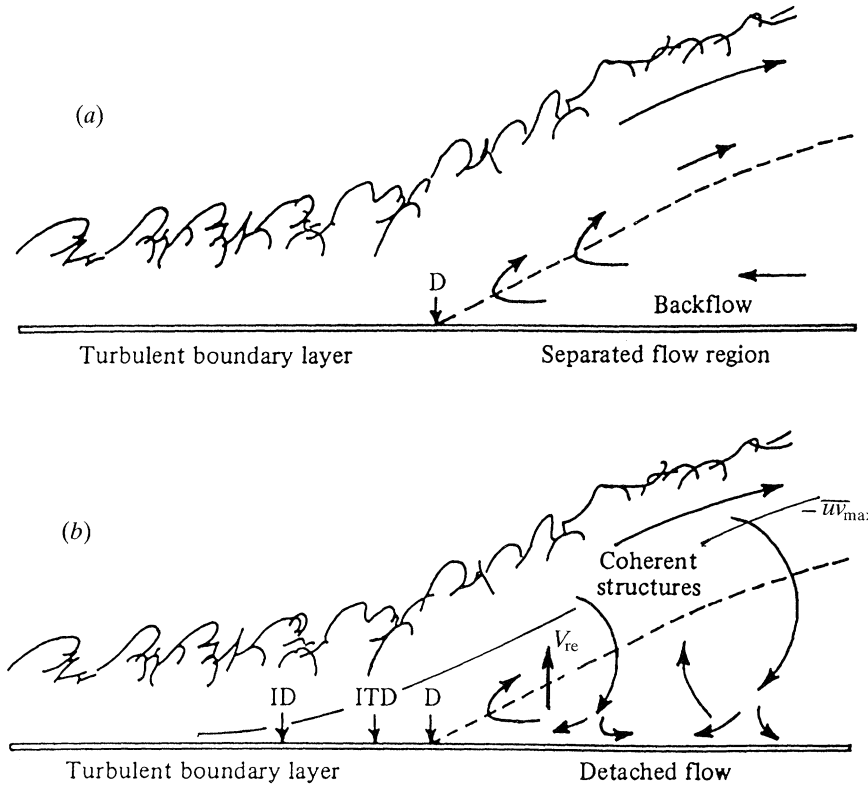

Figure 1. (*a*) Traditional view of turbulent boundary-layer separation with the mean backflow coming from far downstream. The dashed line indicates $U = 0$ locations. (*b*) A flow model with the turbulent structures supplying the small mean backflow. ID, incipient detachment; ITD, intermittent transitory detachment; D, detachment. The dashed line denotes $U = 0$ locations; the solid line denotes maximum turbulent shear location; V_{re} denotes the mean re-entrainment velocity along $U = 0$.

Conversely, the breakdown of the boundary-layer concept can occur before any flow reversal is encountered. In three-dimensional flow the rotational layer can depart without the surface shear stress necessarily falling to zero, and the wall shear is zero only at the singular points.

For steady freestream two-dimensional flows on streamlined surfaces, separation begins intermittently at a given location; that is, the flow reversal at that location occurs only a fraction of the total time. At progressively farther downstream locations, the fraction of time that the flow moves downstream is progressively less. The following set of quantitative definitions on the detachment state near the wall has been proposed and related to earlier nomenclatures (Simpson 1985, 1989), with the definitions based on the fraction of time that the flow moves downstream, γ_{pu} (Simpson 1981): *incipient detachment* (ID) occurs with instantaneous backflow 1% of the time ($\gamma_{pu} = 0.99$); *intermittent transitory detachment* (ITD) occurs with instantaneous backflow 20% of the time ($\gamma_{pu} = 0.80$); *transitory detachment* (TD) occurs with instantaneous backflow 50% of the time ($\gamma_{pu} = 0.50$); and *detachment* (D) occurs where the time-averaged wall shearing stress $\overline{\tau}_w$ is 0. Available data indicate that TD and D occur at the same location.

The length of the region between the ID, ITD, TD and D points will depend on the geometry and the flow, but the definitions of these points are the same (figure 1*b*). γ_{pu} is not a sufficient variable to describe the flow behaviour, because it only represents the fraction of a streamwise velocity probability distribution that is positive. However, it is important that such a feature be documented in all future work.

Relatively little is known about the time-dependent structure of the wall region of separated flows. In the next section the flow behaviour on low-curvature streamlined surfaces is discussed, while a later section deals with flows separating from a backward-facing step with downstream reattachment.

2. Steady free-stream separating turbulent boundary layers

2.1. *Upstream of detachment*

For low-curvature and flat surfaces, the mean flow upstream of ID obeys the 'law of the wall' and the 'law of the wake' as long as the maximum shearing stress, $-\rho\overline{uv}_{\max}$ is less than 1.5 times the wall shear stress τ_{W}. When $-\rho\overline{uv}_{\max} > 1.5\tau_{\mathrm{W}}$, the Perry & Schofield (1973) mean-velocity profile correlation, the law of the wall, and the Ludwieg–Tillman skin-friction equation apply upstream of ITD. The qualitative turbulence structure is not markedly different from the zero-pressure-gradient case, except that the maximum fluctuations are in the middle of the boundary layer near $y/\delta \approx \frac{1}{2}$.

The characteristic frequency f_{b} of the most energetic eddies (frequency of peak energy bandwidth of $fF(f)$ for spectrum $F(f)$) near the wall is correlated by $U_{\mathrm{e}}/f_{\mathrm{b}}\,\delta = 10 \pm 3$, where U_{e} is the mean velocity outside the boundary layer and δ is the boundary layer thickness (Simpson *et al.* 1977). From hydrogen bubble flow visualization in water, Lu *et al.* (1987) report an average period T_{B} of a cycle observed high speed and low speed streaks to be $T_{\mathrm{B}}\,U_{\mathrm{e}}/\delta = 12$, which is close to the result obtained by Simpson *et al.* Their momentum thickness Reynolds number was near 500 whereas Re_θ was less than 14000 upstream of ID for the Simpson *et al.* flow. Lu *et al.* report that the low speed streak usually has a much longer duration than a high speed streak. A rapid thickening of the low speed streak is followed by a violently chaotic ('bursting') short duration vertical motion, which is then blown downstream and replaced by a new high speed streak.

Lu *et al.* observed that spanwise velocity distributions either inside a low speed streak or inside a high speed streak is relatively uniform. Abrupt changes of velocity occur only in a narrow region between a low speed streak and high speed streak. The chaotic vertical motion and longest streamwise streaks originate in this region and extend far downstream.

The low speed streak is not symmetrical in general. On one side of the low speed streak the transition to the high speed streak takes place gradually and $\partial U/\partial z$ is not very large, while on the other side $\partial U/\partial z$ becomes very large and a long streamwise streak originates along this side. The formation of a vertical structure with generation of chaotic flow and 'bursting' takes place along this side of the flow speed streak. Unfortunately, no quantitative values were reported.

Simpson *et al.* (1977) report that the average spanwise spacing of near wall eddies λ_z is approximately constant upstream of ITD. Because $U_\tau = \sqrt{(\tau_{\mathrm{w}}/p)}$ strongly decreases as detachment is approached, the non-dimensional spacing $\lambda_z^+ = \lambda_z U_\tau/\nu$ also strongly decreases. Figure 2 shows λ_Z^+ as a function of the dimensionless pressure-

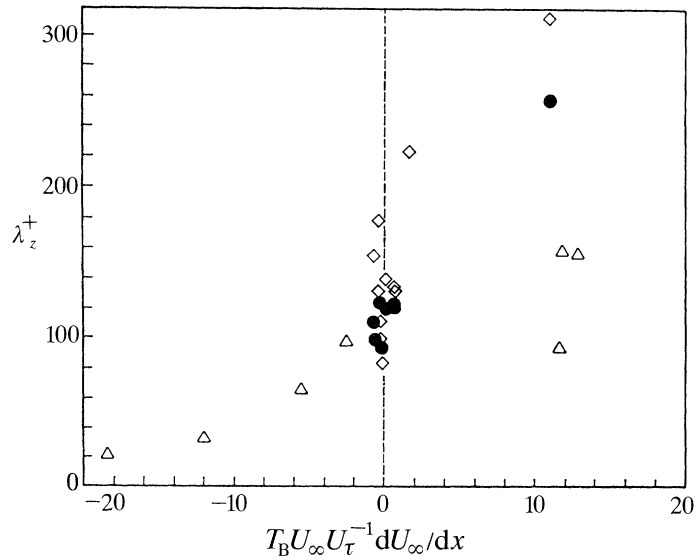

Figure 2. Variation of λ_z^+ with pressure gradient: ●, visual results of Kline *et al.* (1967); ◇, correlation results of Kline *et al.* (1967); △, results of Simpson *et al.* (1977) for attached flows; ▲, results of Simpson *et al.* (1977) for backflow.

gradient parameter. An argument can be put forward for the characteristic dimensionless parameter used here which makes the spread in observed λ_Z^+ values with pressure gradient plausible. The speed of the wall eddies is *ca.* $14U_\tau$, so that $U_\tau T_B$, where T_B is the period $1/f_B$, is proportional to the average streamwise spacing of these eddies. The ratio of the stresses acting in the wall region should also influence the spanwise structure, so that $\tau_w^{-1}\,dP_\infty/dx$ is the ratio of these stresses per unit length. Thus

$$\frac{-U_\tau T_B}{\tau_w}\frac{dP_\infty}{dx} \quad \text{or} \quad \frac{T_B U_\infty}{U_\tau}\frac{dU_\infty}{dx} = P_T$$

constitutes a non-dimensional parameter describing the relative influence of the pressure gradient and the wall shear on each eddy which passes by. The pressure gradient plays an increasing role as separation is approached, since λ_Z^+ decreases from its zero-pressure-gradient value of about 100 with increasingly negative values of P_T. After detachment, λ_Z increases by almost an order of magnitude and the backflow near the wall is subjected to a weak favourable pressure gradient, since dU_∞/dx is still negative. These λ_Z^+ values are shown for a positive P_T and take on magnitudes near 100. The uncertainty in the mean wall shear values and the pressure gradient may be relatively large at these latter stations, contributing to some uncertainty in λ_Z^+ and P_T.

Also shown on figure 2 are the λ_Z^+ results of Kline *et al.* (1967), which are the only other published results available for flows with a non-zero pressure gradient. With exception of the results for strongly accelerating flow, most of their data were obtained at low P_T values. Although there is considerable scatter in their results, a curve passing through the few data points from Simpson *et al.* (1977) for $P_T < 0$ would intersect the centre of their data at $P_T = 0$. In terms of the pressure-gradient

parameter $K = (\nu \, \mathrm{d}U_\infty/\mathrm{d}x)\, U_\infty^{-2}$, the data for their flow with a strong adverse pressure gradient have values of the order of -10^{-6} whereas the present data had values of about -2×10^{-7}. Thus one cannot see any trend of the influence of pressure gradient using this parameter. Although their mean velocity profiles matched the outer-region correlation of Perry & Schofield, no shear-stress profiles were available for examination. Their momentum-thickness Reynolds number was an order of magnitude smaller than for the Simpson *et al.* (1977) flow; $\frac{1}{2}C_f$ was about twice as large so their flow was not near separation. Thus P_T seems to be one parameter which permits a monotonic variation of λ_Z^+ with pressure gradient up to detachment. It should be noted that if one scales λ_Z on $U_M = \sqrt{(-\overline{uv}_{\max})}$, which is an important velocity scale near separation, then $\lambda_Z U_M/\nu$ has values around 110. This suggests that the maximum shearing stress should be used to non-dimensionalize λ_Z, making $\lambda_Z U_M/\nu$ a more general parameter for the wall spanwise structure upstream of separation with a value of about 110, in close agreement with the zero pressure gradient flow value of 100.

2.2. *During detachment and downstream*

As a turbulent boundary layer undergoes an adverse pressure gradient, the flow near the wall decelerates until some backflow first occurs at incipient detachment. A spanwise line of detachment does not move up and downstream as a unit. Small three-dimensional elements of flow move upstream for a distance and are later carried downstream. These reversed flows occur in regions of low kinetic energy and are caused by forces arising from the large-scale structures and the adverse pressure gradient. Large eddies, which bring outer-region momentum toward the wall, intermittently supply some flow in the downstream direction even close to the wall. These large eddies grow rapidly in all directions and agglomerate with one another to decrease the average frequency of passage as detachment is approached. Even through detachment, $U_e/f_b\,\delta \approx 10$ as for attached flow. Substantial pressure-gradient relief begins near intermittent transitory detachment as the detaching shear layer grows at a rate proportional to δ^2.

These large-scale structures supply the turbulence energy to the near-wall detaching flow. The velocity fluctuations in the backflow region are greater than or at least comparable with the mean backflow velocities. Intermittent backflow occurs as far away from the wall as the maximum shearing-stress location $y/\delta > \frac{1}{2}$. Because the free-stream flow is observed to be rather steady, this means that the near-wall fluctuations are not mainly due to a flapping of the entire shear layer, but rather to turbulence within the detached flow. In such a high-turbulence-level flow, mean streamlines do not represent the average pathlines for elements of fluid (figure 1*b*). Even though the outer-region mean-velocity profiles look like those for a free mixing layer, the inner region is substantially different. Mean-velocity profiles and their shape factors $H\,(=\delta^*/\theta)$ are almost independent of momentum-thickness Reynolds number, strongly correlate on γ_{pu} near the wall, and strongly depend on local turbulence conditions (Simpson 1985).

The mean backflow appears to be just large enough to satisfy continuity requirements. The backflow mean velocity U scales on the maximum negative velocity U_N and its distance from the wall, N, which varies with the shear-layer thickness δ. Downstream of detachment the mean backflow can be divided into three layers: a viscous layer nearest the wall that is dominated by the turbulent-flow unsteadiness but with little Reynolds shearing-stress effects; an intermediate layer

PHILOSOPHICAL TRANSACTIONS OF THE ROYAL SOCIETY A MATHEMATICAL, PHYSICAL & ENGINEERING SCIENCES

with a semilogarithmic mean-velocity profile that seems to act as an *overlap region* between the viscous wall and outer regions; and the outer backflow region that is really part of the large-scale outer-region flow. No 'law-of-the-wall' type of velocity profile based on a wall shearing stress is valid for the backflow when $\gamma_{pu} > 0$ and $-\overline{uv} \approx 0$ in the backflow. Agarwal & Simpson (1990) show that this is the case when $U_N/U_e < \frac{1}{4}$. For downstream of detachment ($\gamma_{pu} < \frac{1}{2}$ near the wall), Simpson (1983) presented the equation

$$U/|U_N| = A(y/N - \ln|y/N| - 1) - 1, \tag{1}$$

where $A = 0.3$. This equation describes for a number of data-sets (Agarwal & Simpson 1990) the velocity profile of the middle region of the mean backflow ($0.02 < y/N < 1.0$, where $N/\delta \leqslant 0.06$). Farther away from the wall ($y/N > 1.0$) this equation does not describe the mean-velocity profile well, because this outer backflow region is influenced strongly by the large-scale outer-region flow. Nearer the wall ($y/N < 0.02$), the viscous layer can be described by

$$\frac{U}{|U_N|} = -C\left(\frac{y}{N}\right) + \tfrac{1}{2}P_1\left(\frac{y}{N}\right)^2, \quad \text{where} \quad p_1 = \frac{N^2}{\rho\nu|U_N|}\frac{\mathrm{d}P}{\mathrm{d}x}, \tag{2}$$

and C is a constant. For these flows $P_1 < 125$ and the pressure-gradient term contributes little. Here $|U_n|/U_e$ varies almost linearly with l/H, being zero at $H = 3.5$ and 0.15 at $H = 10$ (Simpson & Shivaprasad 1983). Buckles *et al.* (1984) indicate that their backflow profiles agree with equation (1). Dianat & Castro (1986) also report that equation (1) fits their data, but with $A = 0.235$.

Near detachment and downstream, the large eddies produce $\overline{w^2} = \overline{v^2}$ away from the wall and in the outer region. As a large structure the order of δ in height and width supplies fluid toward the wall in the separated region, v fluctuations decrease and are exactly zero at the wall. Because of continuity requirements, this fluid must be deflected and must contribute to u and w fluctuations. Thus, r.m.s. fluctuations u' and w' are a little greater owing to this wall effect than they would be with large-scale structure effects alone. This explains why u' and w' distributions have the inflection points near the wall. Semilogarithmic profiles of $\overline{u^2}$ and $\overline{w^2}$ between inflection points suggest an overlap region between inner and outer velocity and length scales. No plausible explanation of these data appears possible when elements of fluid in the mean backflow are required to come from far downsteam (figure 1*a*).

Even though $-\overline{uv}$ is relatively large in the outer region, $-\overline{uv}/u'v'$ and $-\overline{uv}/q^2(q^2 = \overline{u^2} + \overline{v^2} + \overline{w^2})$ decrease during the separation process and downstream. In the backflow region these correlations are close to zero. The Reynolds shearing stresses must be modelled by relating them to the turbulence structure and not to local mean-velocity gradients. The mean-velocity profiles in the backflow are a result of time-averaging the large turbulent fluctuations and are not related to the cause of the turbulence. The inertial subrange of velocity spectra of the outer-region forward flow scale on the maximum shear stress at a given streamwise location, as shown by Simpson *et al.* (1990). The most energetic frequencies f in the backflow occur in the range $10 \leqslant U_e/\delta f \leqslant 50$ (Simpson *et al.* 1981*b*).

In the backflow the spanwise structural spacing λ_z of good (significantly positive) cross-correlations in the backflow scales on the local wall shear stress in $\lambda_z U_\tau/\nu$ as shown in figure 2. λ_z/δ is between $\frac{1}{20}$ and $\frac{1}{10}$ for these data. The spanwise spacing with good cross-correlations occurs for 2 to 3 spanwise spacing cycles and indicates that

the large eddies of length scale δ impress this structure simultaneously across the flow.

Normal-stress effects contribute significantly to the momentum and turbulence-energy equations. Negligible turbulence-energy production occurs in the backflow. Normal- and shear-stress production in the outer region supply turbulence energy in the backflow by turbulent diffusion. Movies of laser-illuminated smoke also have clearly revealed that the large-eddy structure supplies most of the near-wall backflow. Fluid elements of the small mean backflow do not come from far downstream, as suggested in figure 1*a*; rather, they appear to be supplied intermittently by large-scale structures as they pass through the separated flow, as suggested by figure 1*b*. Blockage of the backflow region far downstream of detachment does not seem to affect the detachment location (Simpson *et al.* 1981*b*).

Both the turbulence and mean-shear interaction and the turbulence–turbulence interaction in the pressure fluctuation of source term σ of the Poisson equation $\nabla^2 p = -\rho\sigma$ are important for detached flows. Velocity fluctuations are as large as mean velocities in the backflow. Reynolds shear stresses and their gradients are large away from the wall. Thus, the large pressure fluctuations are not at the wall in a detached flow, but rather they must be near the middle of the shear layer. These large pressure fluctuations strongly influence the near-wall flow. $p(x)/\tau_M$ on the wall must decrease if the source σ moves away from the wall. The distance from the wall to the maximum shear location M increases rapidly downstream of detachment and inversely correlates with the decrease in p'/τ_M (Simpson *et al.* 1987).

The coherence of the pressure-fluctuation-producing motions remains high in the streamwise direction upstream of incipient detachment but drops drastically with the beginning of intermittent backflow. The streamwise coherence level downstream of detachment looks much like that for the spanwise direction for attached flows. This indicates that even over small streamwise distances, the detached-flow pressure-fluctuation-producing turbulent motions do not retain the same structural features.

At low frequencies, both upstream and downstream of detachment, U_c celerity of the pressure fluctuations increases with increasing frequency until near $\omega\delta^*/U_\infty =$ 0.5 to 1, as observed by Simpson *et al.* (1987) and Brooks & Hodgson (1981). Upstream of detachment, U_c decreases at high frequencies. Downstream of the beginning of intermittent backflow, the instantaneous wave speed U_c can be both positive and negative for sufficiently high frequencies. Thus the long-time-averaged U_c is lower than at upstream for these frequencies.

The intermittently forward flow ($\gamma_{pu} > 0$) in the mean-backflow region can be due to only two effects. Either high-momentum forward flow moves toward the wall or high-momentum turbulent motions away from the wall set up instantaneous streamwise pressure gradients that are impressed onto the low-momentum wall region to produce instants of forward flow. Both of these effects contribute to the turbulent diffusion of energy, which is consistent with the conclusion given by Simpson *et al.* (1981*b*) that turbulent diffusion and dissipation are the main terms in the backflow turbulence-energy balance. Space-time correlations in the backflow indicate y length scales of the order of δ (Chehroudi & Simpson 1985).

The flow studied by Buckles *et al.* (1984) also supports this view. Visualization of separated flow using surface-injected dye streaks (Zilker & Hanratty 1979) showed the separated shear layer rolling up into vortices that fill the backflow zone. In contrast, if this region behaved as a free shear layer, we would expect instead to see more isolated eddy structures with a passive fluid in the reversed-flow zone

PHILOSOPHICAL TRANSACTIONS OF THE ROYAL SOCIETY A MATHEMATICAL, PHYSICAL & ENGINEERING SCIENCES

separating the shear layer from the surface (Buckles *et al.* 1984). The photographs of Zilker showed columnar motions carrying dye between the surface and the shear layer. Some of the dye columns correspond to strong, intermittent downward motions.

The data of Buckles *et al.* (1984) suggest a qualitative picture of the flow in which shear-layer vortices send fluid downward toward the wall and entrain fluid from the reversed-flow region upward into the shear layer. Large, positive skewness values and large flatness values (Simpson *et al.* 1981*b*) in the reversed-flow region near the wall imply intermittent pulses of forward-moving fluid, possibly associated with the passage of shear-layer vortices overhead. These observations led Buckles *et al.* to suggest that the detached shear flow was driven by a mechanism other than just the external pressure gradient.

Agarwal & Simpson (1990) showed that this driving mechanism is the re-entrainment of backflow into the downstream moving fluid by turbulent diffusion. Note that the mean re-entrainment velocity V_{re} along the $U = 0$ line (figure 1*b*) is related to the mean backflow by the continuity equation

$$\int_{X_{\mathrm{D}}}^{X} V_{\mathrm{re}}\,\mathrm{d}x = \int_{0}^{y_0} U\,\mathrm{d}y,$$

where X_{D} is the location of detachment and y_0 is the location of the $U = 0$ line. V_{re} is governed by large-eddy diffusion, being approximately $\overline{vq^2}/\overline{q^2}$, although data on pressure diffusion $\overline{pv}$ are not available to estimate its likely substantial contribution. Because $\overline{vq^2}$ is positive, this implies that first and second quadrant fluctuations ($v > 0$) must be dominant.

Of course, this mechanism for supplying the backflow may be dominant only when the thickness of the backflow region is small as compared with the turbulent shear-layer thickness, as in the Simpson *et al.* (1981*a*) flow. Experiments (Fox & Kline 1962; Patrick 1987) on separation in wide-angle diffusers indicate that the mean backflow can come mainly from downstream when the thickness of the backflow region is comparable to the thickness of the forward flow, although even in this case $\gamma_{pu} > 0$ in much of the backflow. Thus some forward flow is supplied to the near-wall region by the large eddies, with direct inrushes of forward flow and/or instantaneous favourable pressure gradients imposed on the wall region by the large eddies.

3. The nature of the backward-facing step reattachment

3.1. *Time-mean behaviour*

Although the backward-facing step is the simplest reattaching flow, the flow field is still very complex. Figure 3 illustrates some of the complexities. The upstream boundary layer detaches at the sharp corner, forming a free-shear layer. If the boundary layer is laminar, transition begins soon after detachment, unless the Reynolds number is very low.

The separated shear layer appears to be much like an ordinary plane-mixing layer through the first half of the separated-flow region. Here the divided *mean*-flow streamline is only slightly curved, and the shear layer is thin enough that it is not affected by the presence of the wall (figure 3). However, this shear layer differs from the plane-mixing layer in one important aspect: the flow on the low-speed side of the shear layer is highly turbulent, as opposed to the low-turbulence-level stream in a typical plane-mixing layer experiment.

PHILOSOPHICAL TRANSACTIONS OF THE ROYAL SOCIETY A MATHEMATICAL, PHYSICAL & ENGINEERING SCIENCES

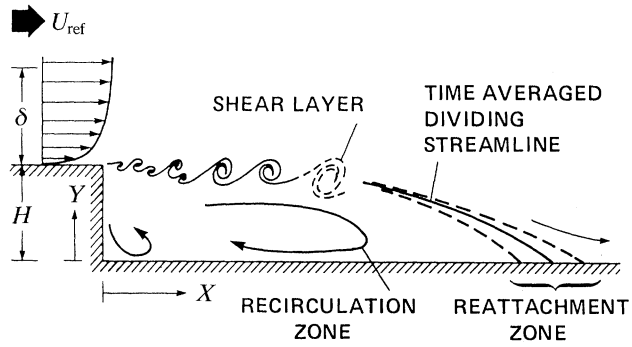

Figure 3. Features of a rearward-facing step flow (Driver *et al.* 1987).

The separated shear layer curves sharply downward in the reattachment zone and impinges on the wall, although any stabilizing effect of curvature appears to be small (Castro & Haque 1987). Part of the shear-layer fluid is deflected upstream into the recirculating flow by a strong adverse pressure gradient. The shear layer is subjected to the effects of adverse pressure gradient and strong interaction with the wall in the reattachment zone. A rapid decay of Reynolds normal and shear stress occurs within the reattachment zone.

The recirculating flow region below the shear layer cannot be characterized as a dead-air zone. The maximum measured backflow velocity is usually over 20% of the free-stream velocity, and skin-friction coefficients as large as $C_f = -0.0012$ (based on the free-stream velocity) have been measured (Adams & Johnston 1988).

The distance from the step to the reattachment location X_R, where $\gamma_{pu} = 0.5$ and $C_f = 0$, is an important length scale for normalizing the streamwise position in correlations of C_f, γ_{pu}, surface pressure coefficient C_p, and pressure fluctuation data. The turbulent-flow reattachment length to step-height ratio X_R/H is mainly a function of the expansion ratio (downstream flow height/upstream flow height = h_2/h_1) for step-height Reynolds numbers Re_H (based on the upstream free-stream velocity and the step height) above 10^4. There is a strong Reynolds number dependence for $Re_H < 6000$. For $h_2/h_1 > 2$, there is little expansion-ratio dependence. X_R/H seems to increase with increasing initial-momentum-thickness Reynolds number and with increasing adverse pressure gradients. When the reattachment surface is divergent from the upstream flow, X_R/H increases. This is plausible, because the large-scale structures of the shear layer must travel farther in order to interact with the reattachment surface. X_R/H can be reduced by a curved edge on the backward-facing step.

Eaton & Johnston (1981) summarize other flow effects on reattachment length. High-free-stream-turbulence levels reduce the reattachment length, as do low-aspect-ratio test channels (width/step height less than 10). Rotation of the channel about a spanwise axis in the stabilizing direction reduces the three-dimensional turbulence and increases the reattachment length about 8% over the no-rotation case. Rotation in the opposite direction enhances the three-dimensional motions and decreases the reattachment length by 50%.

The maximum Reynolds shearing stress occurs near the maximum $\partial U/\partial y$ value, as in detaching flows, and moves toward the wall as re-attachment is approached.

According to Pronchick's (1983) data, the shear correlation coefficient $-\overline{uv}/u'v'$ is about 0.5 in the middle of the detached shear layer, decreasing toward the wall and the free stream. The data of Simpson *et al.* (1981*a*) for a detaching flow show a much lower value. Pressure fluctuations scale on the maximum shearing stress.

The mixing-length and eddy-viscosity ($\epsilon_m/U_e\delta^*$) distributions for the detached flows of Driver & Seegmiller (1985) and Pronchick (1983) have maximum values of about one half those for an attached flow. This is in agreement with the results of Simpson *et al.* (1981*a*). The Reynolds-normal-stress terms of the momentum and turbulent-kinetic-energy equations appear to be important to these flows. Little diffusion of turbulence energy occurs in the backflow before the reattachment region is reached ($\partial\gamma_{pu}/\partial x > 0$). In the backflow as reattachment is approached, the turbulence energy is supplied by diffusion and is balanced by dissipation, because the production and advection terms are negligible. This behaviour is consistent with that for detaching flows.

Downstream of reattachment, the Reynolds stresses continue to decay rapidly for a distance of several step heights. Simultaneously, a new sub-boundary layer begins to grow up through the reattached shear layer. The measurements have shown that the outer part of the reattached shear layer still has most of the characteristics of a free-shear layer as much as 50 step heights downstream of reattachment. This observation demonstrates the persistence of the large-scale eddies that are developed in the separated free-shear layer.

3.2. *Temporal and spatial structure*

This flow is highly unsteady. Large turbulent structures with length scales at least as large as the step height pass through the reattachment region. In addition, flow visualization showed that the length of the separation region fluctuated so that the instantaneous impingement location of the shear layer moved up and downstream. Quantitative measurements confirmed this conclusion and showed that the short-time-averaged reattachment location deviated from the long-time-averaged reattachment location by as much as ± 2 step heights.The non-dimensional frequency of this motion is $fX_R/U_0 \approx 0.6$–0.8, which agrees with the results of Driver *et al.* (1987). Maximum energy content of wall pressure fluctuations occurs at these frequencies. Here X_R is the distance from the step to the long-time-average location of reattachment, and U_0 is the inviscid-flow velocity upstream of the step.

This period between flow reversals in the reattachment region appears to be random with no apparent correlation between the near-wall flow upstream and downstream of reattachment. Although the time T between flow reversals is such that $X_R/TU_0 \approx 0.09$, these flow reversals are short-lived during time t, with $X_R/tU_0 \approx 0.6$ (Driver *et al.* 1987).

The turbulence-intensity level of the detached flow is 5–10% higher than for the plane-mixing layers, which is believed to be the result of a very low frequency ($fX_R/U_0 < 0.1$) vertical or 'flapping' motion of the reattaching shear layer. Streamlines of the flow field at various times in a flapping sequence show that the amplitude of flapping is less than 20% of the shear-layer thickness, and that the flapping correlates with strong flow reversals in the vicinity of reattachment. There is a reduction in the reverse-flow rate with abnormally short instantaneous reattachment lengths. The shear stress in the flow increases dramatically with longer instantaneous reattachment lengths. Driver *et al.* (1987) suggest that the flapping is produced when a particularly high-momentum structure moves far downstream

PHILOSOPHICAL TRANSACTIONS OF THE ROYAL SOCIETY A MATHEMATICAL, PHYSICAL & ENGINEERING SCIENCES

before reattaching. This would create a somewhat greater pressure gradient that would cause greater backflow at a later time. The flapping motion produces negligible contributions to the Reynolds shearing stress.

Adams & Johnston (1988) reported near wall turbulent 'burst' rates from hot-wire anemometer data at X^* ($X^* = (X - X_R)/X_R$) of -0.38 and -0.58 where $\gamma_{pu} \approx 0$. They used the Blackwelder & Kaplan (1976) VITA technique to extract the 'burst' frequency f_B, which was observed to decrease away from the wall according to $f_B \nu / U_\tau^2 = 0.01 y^{+-0.9}$.

They suggested several reasons why the increased detection rate inside of $y^+ = 20$ is probably the result of properties of the VITA technique and does not represent an increase in the near-wall production mechanism. First, there is no observed rise in $\overline{u'^2}$ in the near-wall region, as would be expected if turbulent shear stress were being produced. Second, there is little vertical movement of these structures as in a 'normal' boundary layer, since burst-detection rates fall rapidly with increasing y^+ in the near-wall zone. Third, the values of y^+ are so small in the region of higher detected burst rates that even in a normal boundary layer viscous effects would dominate.

They concluded that while the measured bursting rates in the upstream attached boundary layer agree very closely with those measured for a zero pressure gradient turbulent boundary layer, the detection rates in the backflow region are a factor of 4–10 lower. The lack of bursting in the near-wall region is the reason for the lack of the $-\overline{uv}$ correlation noted by Simpson *et al.* (1981*a*) and by Pronchick (1983). The diminished bursting rates occur both under favourable pressure-gradient and adverse pressure-gradient conditions.

The largest structure in the flow originates from the roll-up and multiple pairing of spanwise vortices (Pronchick 1983). This roll-up is similar to the vortex roll-up and pairing process seen in the plane free-shear layer. The convective speed of these structures is about $0.6U_0$. The spanwise coherence or organization of these vortical structures starts to break down about three step heights downstream of detachment. The turbulence structure becomes fully three-dimensional upstream of reattachment.

From their flow visualization studies, Müller & Gyr (1982) explained this breakdown behaviour conceptually. As soon as a vortex tube is bent or distorted, it starts to induce velocities on itself (the Biot–Savart law). A vortex loop bent in the downstream direction moves away from the adjacent wall, while a vortex loop bent in the upstream direction moves closer toward the wall. The velocity induced on the near-wall vortex loop by its image vortex can cause it to move upstream relative to the surrounding flow, thus supplying some backflow and forming a very large streamwise lengthscale and a long timescale. The vortex tubes that are stretched in the streamwise direction lead to more intense mixing, greater Reynolds shearing stresses, and greater turbulence intensities.

In his hydrogen bubble flow visualization studies, Pronchick (1983) did not observe only large-scale structures in the backflow zone. Instead, he found that the backflow consists of small-scale streak-like turbulent fluid created by large eddy impingements on the wall and directed upstream by the adverse pressure gradient. This is not inconsistent with the conceptual description of Müller & Gyr (1982), which deals with the outer region upstream of reattachment.

Pronchick examined the spanwise spacing between smaller-scale streaks. The fluctuations in spanwise velocity near the wall appear much higher than in the

PHILOSOPHICAL TRANSACTIONS OF THE ROYAL SOCIETY A MATHEMATICAL, PHYSICAL & ENGINEERING SCIENCES

attached boundary layer upstream of the step. At $X^* = -0.37$ and $X^* = 0.22$, he reported λ_z^+ to be about 54 and 59, respectively. At these locations C_f and γ_{pu} near the wall are about -10^{-3} and 0.01, and 0.6×10^{-3} and 0.9, respectively. The upstream location was close to where C_f was the greatest for the backflow; the second location was downstream of reattachment. Both locations had intermittently forward flow.

Pronchick suggested that the remaining presence of large eddies may be responsible for these relatively low values of λ_z^+ as compared to the attached boundary layer value of 100. When large eddies impinge on the wall, they may tend to reverse the prevailing flow direction near the wall, resulting in instantaneous values of wall shear stress which are opposite in sign from the near wall shear stress. Of course, the detached flow of Simpson *et al.* (1977) should also be subject to similar large eddies effects, but λ_z^+ values were closer to 100 than Pronchick's results.

4. Conclusions

The structure of the near wall region of nominally two-dimensional turbulent separating, separated, and reattaching flows is considerably different from that of an attached turbulent boundary layer. Local flow direction reversal, low mean velocities, high turbulence intensities, and the dominance of outer-region large-scale structures are characteristic features. Negligible turbulence energy production and Reynolds stress $-\overline{uv}$ near the wall and the importance of turbulence energy diffusion toward the wall support the view that the near-wall region structures do not yield stress-producing 'bursts'. A streamwise streaky structure seems to be impressed on the wall region by the outer flow, but scales crudely on the wall shear stress, $\lambda_z^+ \approx O(10^2)$. While additional experimental data on such features may clarify the detailed structure, it is unlikely that the qualitative discussion and conclusions presented here will change.

References

Adams, E. W. & Johnston, J. P. 1988 Flow structure in the near-wall zone of a turbulent separated flow. *AIAA Jl* **26**, 932–939.

Agarwal, N. K. & Simpson, R. L. 1990 The backflow structure of steady and unsteady separating turbulent boundary layers. *AIAA Jl* **28**, 1764–1771.

Blackwelder, R. F. & Kaplan, R. E. 1976 On the wall structure of the turbulent boundary layer. *J. Fluid Mech.* **76**, 89–112.

Brooks, T. F. & Hodgson, T. H. 1981 Trailing edge noise prediction from measured surface pressures. *J. Sound Vib.* **78**, 69–117.

Buckles, J., Hanratty, T. J. & Adrain, R. J. 1984 Turbulent flow over large-amplitude wavy surfaces. *J. Fluid Mech.* **140**, 27–44.

Castro, I. P. & Haque, A. 1987 The structure of a turbulent shear layer bounding a separation region. *J. Fluid Mech.* **179**, 439–468.

Chehroudi, B. & Simpson, R. L. 1985 Spacetime results for a separating turbulent boundary layer using a rapidly scanning laser anemometer. *J. Fluid Mech.* **160**, 77–92.

Dianat, M. & Castro, I. P. 1986 Measurements in separating boundary layers using pulsed wire anemometry. *ICAS-86-1.7.2, 15th Congr. Int. Counc. Aerosp. Sci., London.*

Driver, D. M. & Seegmiller, H. L. 1985 Features of a reattaching turbulent shear layer in divergent channel flow. *AIAA Jl* **25**, 163–171.

Driver, D. M., Seegmiller, H. L. & Marvin, J. 1987 Time-dependent behavior of a reattaching shear layer. *AIAA Jl* **25**, 914–919.

Eaton, J. K. & Johnston, J. P. 1981 A review of research on subsonic turbulent flow reattachment. *AIAA Jl* **19**, 1093–1100.

PHILOSOPHICAL TRANSACTIONS OF THE ROYAL SOCIETY A MATHEMATICAL, PHYSICAL & ENGINEERING SCIENCES

Fox, R. W. & Kline, S. J. 1962 Flow regimes for curved subsonic diffusers. *J. basic Engng* **84**, 303–312.

Kline, S. J., Reynolds, W. C., Schraub, F. A. & Runstadler, P. W. 1967 The structure of turbulent boundary layers. *J. Fluid Mech.* **30**, 741–773.

Lu, S. J., Lee, C. H., Lian, Q. X., Zhu, Z. Q. & Leng, H. Y. 1987 Recent progress in three-dimensional turbulent boundary layer research at BIAA. *Perspectives in turbulence studies* (ed. H. U. Meier & P. Bradshaw), pp. 414–438. Berlin: Springer-Verlag.

Müller, A. & Gyr, A. 1982 Visualization of the mixing layer behind dunes. *Proc. Euro-mech 156, Mechanics of Sediment-Transport, Istanbul.*

Patrick, W. P. 1987 Flowfield measurements in a separated and reattached flat plate turbulent boundary layer. *NASA CR 4052.*

Perry, A. E. & Schofield, W. H. 1973 Mean velocity and shear stress distributions in turbulent boundary layers. *Phys. Fluids* **16**, 2068–2074.

Pronchick, S. 1983 Experimental investigation of the turbulent flow behind a backward facing step. Ph.D. dissertation. Stanford University, California.

Sears, W. R. & Telionis, D. P. 1975 Boundary-layer separation in unsteady flow. *SIAM J. appl. Math.* **28**, 1.

Simpson, R. L. 1981 A review of some phenomena turbulent flow separation. *J. Fluids Engng* **102**, 520–533.

Simpson, R. L. 1983 A model for the back-flow mean velocity profile. *AIAA Jl* **21**, 142–143.

Simpson, R. L. 1985 Two-dimensional turbulent separated flow. *AGARDograph 287*, vol. 1.

Simpson, R. L. 1987 A review of two-dimensional turbulent separated flow calculation methods. *IUTAM Symp. Boundary Layer Separation, London, 1986* (ed. F. T. Smith & S. N. Brown), pp. 179–196. Berlin: Springer-Verlag.

Simpson, R. L. 1989 Turbulent boundary-layer separation. *A. Rev. Fluid Mech.* **21**, 205–234.

Simpson, R. L., Agarwal, N. K., Nagabushana, K. A. & Ölcmen, S. 1990 Spectral measurements and other features of separating turbulent flows. *AIAA Jl* **28**, 446–452.

Simpson, R. L. & Shivaprasad, B. G. 1983 The structure of a separating turbulent boundary layer. V. Frequency effects on periodic unsteady freestream flows. *J. Fluid Mech.* **131**, 319–339.

Simpson, R. L., Strickland, J. H. & Barr, P. W. 1977 Failures of a separating turbulent boundary layer in the vicinity of separation. *J. Fluid Mech.* **79**, 553–594.

Simpson, R. L., Chew, Y.-T. & Shivaprasad, B. G. 1981*a* The structure of a separating turbulent boundary layer. Part I. Mean flow and Reynolds stresses. *J. Fluid Mech.* **113**, 23–51.

Simpson, R. L., Chew, Y.-T. & Shivaprasad, B. G. 1981*b* The structure of a separating turbulent boundary layer. Part II. Higher order turbulence results. *J. Fluid Mech.* **113**, 53–73.

Simpson, R. L., Ghodbane, M. & McGrath, B. E. 1987 Surface pressure fluctuations in a separating turbulent boundary layer. *J. Fluid Mech.* **177**, 167–186.

Zilker, D. P. & Hanratty, T. J. 1979 Influence of the amplitude of a solid wavy wall on a turbulent flow. II. Separated flows. *J. Fluid Mech.* **90**, 257–271.

PHILOSOPHICAL TRANSACTIONS OF THE ROYAL SOCIETY A MATHEMATICAL, PHYSICAL & ENGINEERING SCIENCES